

Evidence for Γ_8 Ground-State Symmetry of Cubic YbB_{12} Probed by Linear Dichroism in Core-Level Photoemission

Yuina Kanai^{1,2}, Takeo Mori¹, Sho Naimen¹, Kohei Yamagami^{1,2}, Hidenori Fujiwara^{1,2},
Atsushi Higashiya^{2,3}, Toshiharu Kadono^{2,4}, Shin Imada^{2,4}, Takayuki Kiss^{1,2,5},
Arata Tanaka⁶, Kenji Tamasaku^{2,5}, Makina Yabashi²,
Tetsuya Ishikawa², Fumitoshi Iga⁷, and Akira Sekiyama^{1,2,5}

¹*Division of Materials Physics,*

Graduate School of Engineering Science,

Osaka University, Toyonaka, Osaka 560-8531, Japan

²*RIKEN SPring-8 Center, Sayo, Hyogo 679-5148, Japan*

³*Faculty of Science and Engineering,*

Setsunan University, Neyagawa, Osaka 572-8508, Japan

⁴*Department of Physical Sciences,*

Ritsumeikan University, Kusatsu, Shiga 525-8577, Japan

⁵*Center for Promotion of Advanced and Interdisciplinary Research,*
Graduate School of Engineering Science,

Osaka University, Toyonaka, Osaka 560-8531, Japan

⁶*Department of Quantum Matter, ADSM,*

Hiroshima University, Higashi-Hiroshima,
Hiroshima 739-8530, Japan

⁷*College of Science, Ibaraki University,*

Mito, Ibaraki 310-8512, Japan

We have successfully observed linear dichroism in angle-resolved Yb^{3+} $3d_{5/2}$ core-level photoemission spectra for YbB_{12} in cubic symmetry. Its anisotropic $4f$ charge distribution due to the crystal-field splitting is responsible for the linear dichroism, which has been verified by spectral simulations using ionic calculations with the full multiplet theory for a single-site Yb^{3+} ion in cubic symmetry. The observed linear dichroism as well as the polarization-dependent spectra in two different photoelectron directions for YbB_{12} are quantitatively reproduced by theoretical analysis for the Γ_8 ground state, indicating the Γ_8 ground-state symmetry for the Yb^{3+} ions mixed with the Yb^{2+} state.

Rare-earth-based strongly correlated electron systems show various interesting phenomena such as competition between magnetism and unconventional superconductivity, charge and/or multipole ordering, and the formation of a narrow ($\sim\text{meV}$) gap at low temperatures. Among them, YbB_{12} is known as a Kondo semiconductor [1–5], which has been recently recognized as a candidate for topological insulators [6], as intensively discussed for another Kondo semiconductor, SmB_6 [7–9]. The mean valence of YbB_{12} has been estimated as $\sim 2.9+$ by bulk-sensitive $3d$ core-level hard X-ray photoemission (HAXPES) spectroscopy [10]. To discuss the mechanisms of the gap opening at low temperatures [5, 11–16] and the possibility of a topological insulator, it is essential to verify the ground-state symmetry of the Yb^{3+} [$4f^{13}$ (one hole)] state determined by crystalline-electric-field (CEF) splitting. Nevertheless, it is unclear for YbB_{12} . Its eightfold degenerated Yb^{3+} $4f_{7/2}$ levels are considered to split into two quartets [17] (normally, two doublets and a quartet) due to CEF in YbB_{12} . The ground state of the Yb^{3+} ions is commonly asserted to be in the so-called Γ_8 symmetry [5, 18], but a possible accidentally degenerated $\Gamma_6 + \Gamma_7$ ground state is not completely excluded [17]. In this Letter, we show evidence for the Γ_8 symmetry of the Yb^{3+} sites in the ground state of YbB_{12} on the basis of linear

dichroism in *angle-resolved* core-level photoemission.

Generally, it is difficult to experimentally determine the $4f$ ground-state symmetry. Inelastic neutron scattering is useful, but other excitations such as phonon excitations often hamper the observation of magnetic $4f-4f$ excitations. Linear dichroism (LD) in $3d$ -to- $4f$ soft X-ray absorption spectroscopy (XAS) for single crystals is powerful owing to the dipole selection rules, as reported for Ce compounds [19–22]. However, it is not applicable to compounds in cubic symmetry, in which there is no anisotropic axis relative to the electric field of the incident light. On the other hand, the selection rules work also in the photoemission process while the excited electron energy is much higher than that in the absorption. Furthermore, there is another controllable measurement parameter in photoemission, called the “photoelectron detection direction” relative to the single-crystalline axis, in addition to the polarization direction of the excitation light. Indeed, by using LD in $3d$ core-level HAXPES spectra, the Yb^{3+} $4f$ ground state has been determined for tetragonal YbCu_2Si_2 and YbRh_2Si_2 [23]. LD in the core-level HAXPES for cubic Yb compounds is also expected to be observed, as discussed below.

In the case of Yb^{3+} ions in tetragonal symmetry, the eightfold degenerate $J = 7/2$ state splits into four dou-

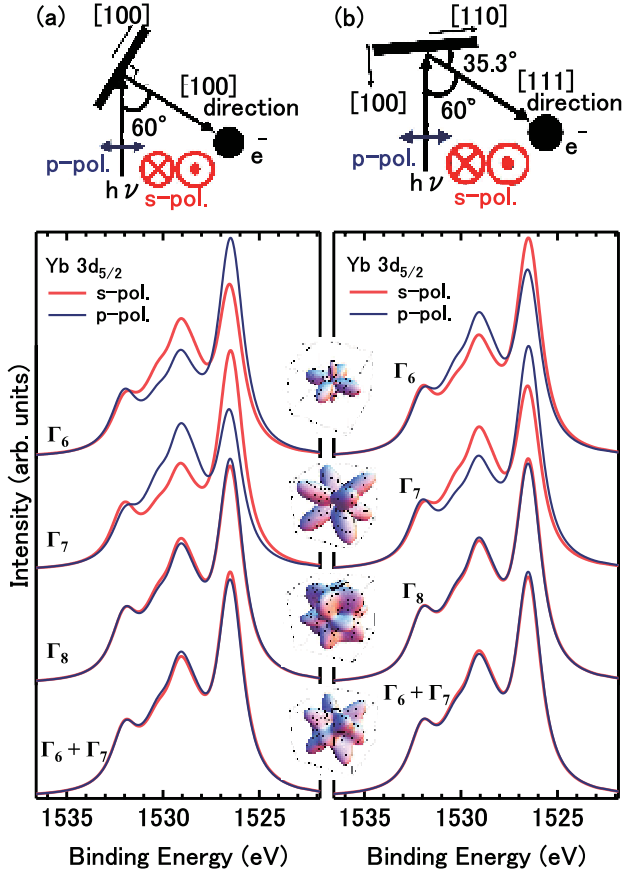


FIG. 1. (Color online) (a) Simulated polarization-dependent $3d_{5/2}$ photoemission spectra of Yb^{3+} ions assuming the crystal-field-split ground state in cubic symmetry in the [100] direction, together with the corresponding experimental geometry. (b) Same as (a) but for the photoelectron in the [111] direction. The $4f$ -hole spatial distributions for the corresponding states are also shown.

plets as

$$|\Gamma_7^1\rangle = c|\pm 5/2\rangle + \sqrt{1-c^2}|\mp 3/2\rangle, \quad (1)$$

$$|\Gamma_7^2\rangle = -\sqrt{1-c^2}|\pm 5/2\rangle + c|\mp 3/2\rangle, \quad (2)$$

$$|\Gamma_6^1\rangle = b|\pm 1/2\rangle + \sqrt{1-b^2}|\mp 7/2\rangle, \quad (3)$$

$$|\Gamma_6^2\rangle = \sqrt{1-b^2}|\pm 1/2\rangle - b|\mp 7/2\rangle, \quad (4)$$

where the coefficients $0 \leq b \leq 1, 0 \leq c \leq 1$ defining the actual charge distributions and CEF splitting energies depend on the CEF parameters $B_2^0, B_4^0, B_4^4, B_6^0,$ and B_6^4 in Stevens formalism [24]. In the cubic symmetry, the eightfold degenerate $J = 7/2$ state splits generally into two doublets and one quartet as

$$|\Gamma_6\rangle = \sqrt{5/12}|\pm 7/2\rangle + \sqrt{7/12}|\mp 1/2\rangle, \quad (5)$$

$$|\Gamma_7\rangle = -\sqrt{3/2}|\pm 5/2\rangle + 1/2|\mp 3/2\rangle, \quad (6)$$

$$|\Gamma_8\rangle = \begin{cases} -\sqrt{7/12}|\pm 7/2\rangle + \sqrt{5/12}|\mp 1/2\rangle \\ 1/2|\pm 5/2\rangle + \sqrt{3/2}|\mp 3/2\rangle \end{cases}. \quad (7)$$

The Γ_6 and Γ_7 states correspond to the tetragonal Γ_6^1 (with $b = \sqrt{7/12}$) and Γ_7^2 (with $c = 1/2$) states, respectively. Since their $4f$ charge distributions deviate from spherical symmetry owing to the CEF splitting even in the cubic symmetry, as shown in Fig. 1, it is natural to expect the observation of LD in core-level photoemission for cubic Yb compounds. The $\Gamma_6, \Gamma_7,$ and Γ_8 $4f$ charge distributions are elongated along the [100], [111], and [110] directions, respectively. Actually, we have performed ionic calculations including the full multiplet theory [25] and the local CEF splitting using the XTLS 9.0 program [26]. All atomic parameters such as the $4f$ - $4f$ and $3d$ - $4f$ Coulomb and exchange interactions (Slater integrals) and the $3d$ and $4f$ spin-orbit couplings have been obtained using Cowan's code [27] based on the Hartree-Fock method. The Slater integrals (spin-orbit couplings) are reduced to 88% (98%) to fit the core-level photoemission spectra [10].

Simulated polarization-dependent $\text{Yb}^{3+} 3d_{5/2}$ core-level HAXPES spectra in cubic symmetry at two photoelectron directions ([100] and [111]) are shown in Fig. 1. In the case of YbB_{12} , since the accidentally degenerated $\Gamma_6 + \Gamma_7$ states could be a candidate for the ground state, the simulations assuming the $\Gamma_6 + \Gamma_7$ ground state and its $4f$ hole spatial distribution are also shown. LD defined by the difference in spectral weight between the s- and p-polarization configurations is reversed between the [100] and [111] directions for all states displayed here. LD for the Γ_6 ground state has the same tendency as that for the Γ_8 ground state. On the other hand, LD for the Γ_8 state is the smallest since the $4f$ hole spatial distribution for the Γ_8 state is the nearest to a spherical shape among these three eigenfunctions. LD assuming the $\Gamma_6 + \Gamma_7$ state is reversed to that for the Γ_8 state. These simulations indicate that the symmetry of the Yb^{3+} state can be determined by LD in the core-level photoemission.

We have performed LD in HAXPES [28, 29] at BL19LXU of SPring-8 [30] using a MBS A1-HE hemispherical photoelectron spectrometer. A Si(111) double-crystal monochromator selected linearly polarized 7.9 keV radiation within the horizontal plane, which was further monochromatized using a Si(620) channel-cut crystal. To switch the linear polarization of the excitation light from the horizontal direction to the vertical direction, two single-crystalline (100) diamonds were used as a phase retarder placed downstream of the channel-cut crystal. The P_L (degree of linear polarization) of the polarization-switched X-ray after the phase retarder was estimated as -0.93 , corresponding to the vertically linear polarization component of 96.5%. Since the detection direction of photoelectrons was set in the horizontal plane with an angle to incident photons of 60° , as shown in Figs. 1(a) and 1(b), the experimental configuration at the horizontally (vertically) polarized light excitation corresponds to the p-polarization (s-polarization). The

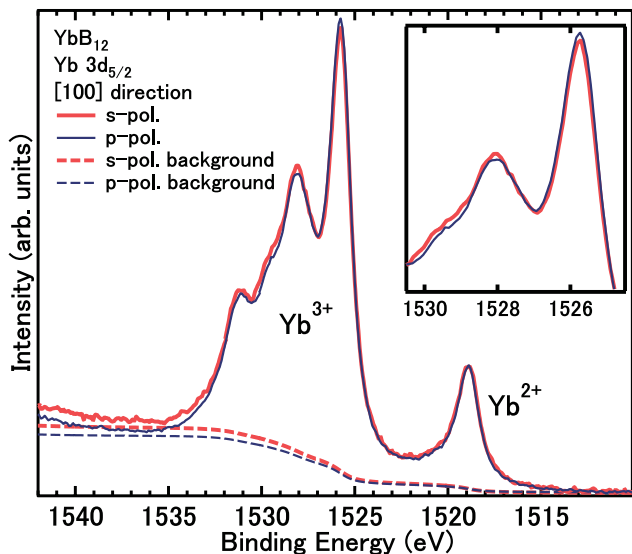


FIG. 2. (Color online) Polarization-dependent Yb $3d_{5/2}$ core-level HAXPES raw spectra (solid lines) of YbB₁₂ in the [100] direction and optimized Shirley-type backgrounds (see text), which we have subtracted from the raw spectra (dashed lines). The raw spectra have been normalized by the Yb²⁺ spectral weight. The same spectra in the expanded scale are also shown.

excitation light was focused onto the samples using an ellipsoidal Kirkpatrick-Baez mirror. To precisely detect LD in the Yb $3d$ core-level photoemission spectra, we optimized the photon flux so as to set comparable photoelectron count rates between the s- and p-polarization configurations. Single crystals of YbB₁₂ synthesized by the traveling-solvent floating-zone method [3, 4] were fractured along the (100) plane *in situ*, where the base pressure was $\sim 1 \times 10^{-7}$ Pa. The experimental geometry was controlled using a newly developed two-axis manipulator [31], where the normal emission direction parallel to the [100] direction in Fig. 1(a) was changed to the photoelectron detection in the [111] direction in Fig. 1(b) by azimuthal rotation of 45° and polar rotation by $\sim 55^\circ$. The sample and surface qualities were examined on the basis of the absence of any core-level spectral weight caused by possible impurities including oxygen and carbon. The energy resolution was set to 400 meV. The measuring temperature is 9 K, which is sufficiently lower than the excited state ($\gtrsim 250$ K) [18].

The polarization-dependent Yb³⁺ $3d_{5/2}$ HAXPES spectra in the [100] direction of YbB₁₂ are shown in Fig. 2. A single peak at a binding energy of ~ 1519 eV and a multiple peak ranging from 1524 to 1534 eV exist in all the spectra. Since the $4f$ subshell is fully occupied in the Yb²⁺ sites with a spherically symmetric $4f$ distribution, the former single peak is ascribed to the Yb²⁺

states. The $3d^9 4f^{13}$ final states for the Yb³⁺ components show an atomic-like multiplet-split peak structure in the 1524 – 1534 eV range. We show the same raw spectra in the expanded scale ranging from 1524.5 to 1530.5 eV in Fig. 2. A slight but intrinsic LD is seen in the highest and second-highest peaks in the raw spectra. The so-called Shirley-type backgrounds are also displayed in Fig. 2. We have optimized the backgrounds as follows: After the normalization of the background-subtracted spectra by both Yb²⁺ and Yb³⁺ $3d_{5/2}$ spectral weights, the relative Yb²⁺/Yb³⁺ contributions and the intensities in the high-binding-energy region of 1534 – 1540 eV become equivalent between the s- and p-polarization configurations. The reference binding energy on the higher side has been set to 1536.2 eV corresponding to the local minimum of the raw spectral weight in the p-polarization. As a result, there are finite spectral weights at ~ 1536 eV in the background-subtracted spectra. However, these should be intrinsic owing to the overlap of the tails of the lifetime-broadened Yb³⁺ $3d_{5/2}$ main peaks and a plasmonic energy-loss structure at the higher binding energy. Note that we have confirmed the robustness of LD in the 1524 – 1531 eV region regardless of background intensity.

A comparison of the polarization-dependent background-subtracted Yb³⁺ $3d_{5/2}$ HAXPES spectra of YbB₁₂ and their LD with the photoelectron directions of [100] and [111] with the simulated ones for the Γ_8 ground state is shown in Fig. 3. The highest peak is slightly stronger in the p-polarization configuration (p-pol.) than in the s-polarization one (s-pol.), and the second highest peak is stronger in the s-pol. for both experimental and simulated spectra in the [100] direction. These tendencies are reversed in the data in the [111] direction. As shown in Figs. 3(a) and 3(b), the observed LD and spectra are quantitatively reproduced by the simulations for the Γ_8 ground state, for which the $4f$ charge distribution is shown in Fig. 3(c). If the $4f$ ground state of YbB₁₂ were in the Γ_6 symmetry, LD would be much larger than the experimental one. The sign of LD for the Γ_7 or accidentally degenerated $\Gamma_6 + \Gamma_7$ ground state is completely inconsistent with our experimental results. Such a quantitative reproducibility of the observed LD and core-level spectra by the simulations surely indicates the Yb³⁺ ($4f^{13}$) ions in the Γ_8 symmetry mixed with a small quantity ($\sim 10\%$) of the Yb²⁺ ($4f^{14}$) component [10] in the ground state of YbB₁₂.

Our finding of the Γ_8 $4f$ symmetry for the Yb³⁺ sites in the ground state is consistent with the prediction by a band-structure (local density approximation + on-site Coulomb repulsion, LDA+ U) calculation, where the Γ_6 and Γ_7 states are on the occupied side [5]. One might consider that the Γ_6 and Γ_7 states are possibly mixed in the ground state due to the hybridization between the $4f$ and valence-band orbitals at low temperatures well below the Kondo temperature (~ 240 K for YbB₁₂ [1–4]). As widely recognized for the local electronic structures of transition metal oxides, on the other hand, note that

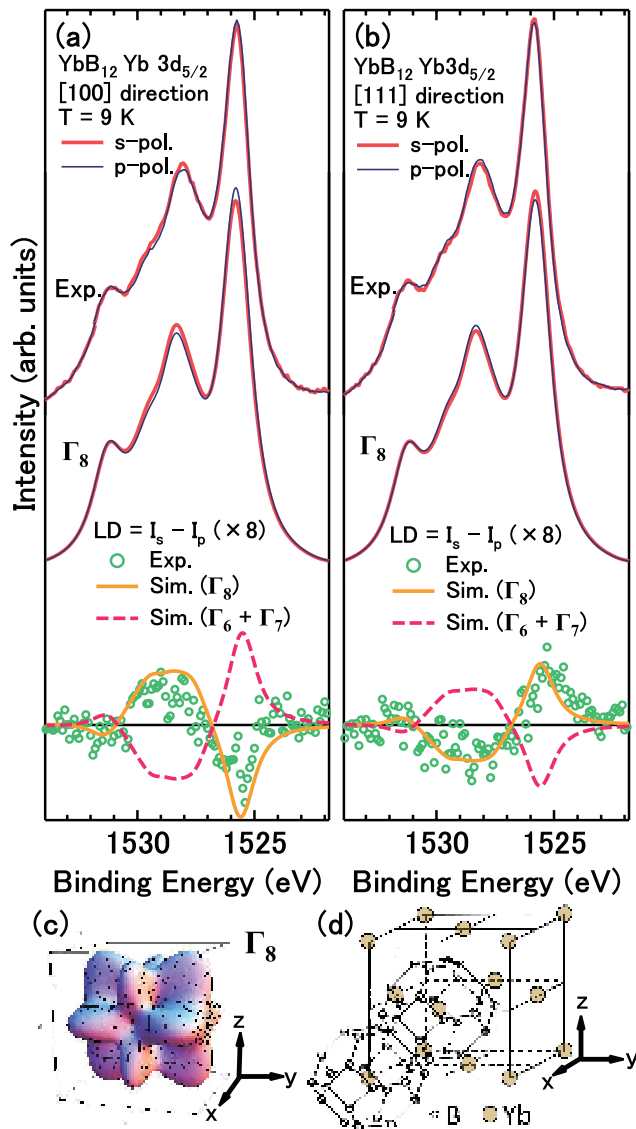


FIG. 3. (Color online) (a) Polarization-dependent $\text{Yb}^{3+} 3d_{5/2}$ core-level HAXPES spectra and LD of YbB_{12} compared with the simulated ones for the Γ_8 ground state in the $[100]$ direction. Simulated LD assuming the accidentally degenerated $\Gamma_6 + \Gamma_7$ ground state is also shown by the dashed line in the lower panel. (b) Same as (a) but data in the $[111]$ direction. The Shirley-type background has been subtracted from the raw spectra (Fig. 2). (c) $4f$ -hole spatial distribution for the Yb^{3+} ion with the Γ_8 symmetry. (d) Crystal structure of YbB_{12} [32]

the so-called CEF splitting actually seen in realistic materials is a consequence of the anisotropic hybridization effects in addition to static ligand potentials. The latter would be much smaller than the former for YbB_{12} since the ligand-field potential on the Yb sites is to some extent nearer to a spherically symmetric one, being caused by the crystal structure [1, 2, 32] where the Yb ion is surrounded by the truncated octahedron made of 24 boron ions as shown in Fig. 3(d). The $4f$ -hole spatial distributions are elongated along the centers of the truncated octahedron faces for the Γ_6 and Γ_7 states, whereas they are elongated along the edges of the hexagonal faces for the Γ_8 state, which leads to the conclusion that the $4f$ holes in the Γ_8 state are relatively stabilized by the hybridizations compared with those in the Γ_6 and Γ_7 states with different symmetries, as suggested by the LDA+ U calculation. Then, the possible Γ_6 and/or Γ_7 state mixture would be experimentally insignificant in our data.

In summary, we have successfully determined the $4f$ symmetry of the Yb^{3+} sites in the ground state for cubic YbB_{12} as the Γ_8 symmetry by LD in the Yb^{3+} core-level HAXPES in two different photoelectron directions. Our result also suggests that the Yb^{3+} ion model under the effective CEF, in which the hybridization effects are implicitly taken into account, is suitable even for the valence-fluctuating system at low temperatures well below the Kondo temperature. The applicability of LD in the core-level HAXPES even to the system in the cubic symmetry (not restricted to systems with lower symmetry) demonstrated here would be promising for revealing the strongly correlated orbital symmetry of the ground state in a partially filled subshell, the charge distribution of which deviates from the spherical symmetry.

ACKNOWLEDGMENTS

We thank H. Yomosa, S. Fujioka, K. Yano, Y. Nakata, Y. Nakatani, T. Yagi, S. Tachibana, Y. Nakamura, H. Aratani, and K. Kodera for supporting the experiments. We are also grateful to K. Miyake, A. Tsuruta, Y. Saitoh, A. Yasui, and A. Fujimori for fruitful discussions. This work was supported by a Grant-in-Aid for Scientific Research (23654121), Grants-in-Aid for Young Scientists (23684027 and 23740240), and a Grant-in-Aid for Innovative Areas (20102003) from MEXT and JSPS, Japan, and by Toray Science Foundation. The hard X-ray photoemission was performed at SPring-8 under the approval of JASRI (2014A1149, 2014B1305).

[1] M. Kasaya, F. Iga, K. Negishi, S. Nakai, and T. Kasuya, *J. Magn. Magn. Mater.* **31-34**, 437 (1983).

[2] M. Kasaya, F. Iga, M. Takigawa, and T. Kasuya, *J. Magn. Magn. Mater.* **47-48**, 429 (1985).

- [3] F. Iga, N. Shimizu, and T. Takabatake, *J. Magn. Magn. Mater.* **177-181**, 337 (1998).
- [4] T. Susaki, Y. Takeda, M. Arita, K. Mamiya, A. Fujimori, K. Shimada, H. Namatame, M. Taniguchi, N. Shimizu, F. Iga, and T. Takabatake, *Phys. Rev. Lett.* **82**, 992 (1999).
- [5] T. Saso and H. Harima, *J. Phys. Soc. Jpn.* **72**, 1131 (2003).
- [6] H. Weng, J. Zhao, Z. Wang, Z. Fang, and X. Dai, *Phys. Rev. Lett.* **112**, 016403 (2014).
- [7] M. Dzero, K. Sun, V. Galitski, and P. Coleman, *Phys. Rev. Lett.* **104**, 106408 (2010).
- [8] T. Takimoto, *J. Phys. Soc. Jpn.* **80**, 123710 (2011).
- [9] S. Suga, K. Sakamoto, T. Okuda, K. Miyamoto, K. Kuroda, A. Sekiyama, J. Yamaguchi, H. Fujiwara, A. Irizawa, T. Ito, S. Kimura, T. Balashov, W. Wulfhchel, S. Yeo, F. Iga, and S. Imada, *J. Phys. Soc. Jpn.* **83**, 014705 (2014).
- [10] J. Yamaguchi, A. Sekiyama, S. Imada, H. Fujiwara, M. Yano, T. Miyamachi, G. Funabashi, M. Obara, A. Higashiya, K. Tamasaku, M. Yabashi, T. Ishikawa, F. Iga, T. Takabatake, and S. Suga, *Phys. Rev. B* **79**, 125121 (2009).
- [11] K. A. Kikoin and A. S. Mishchenko, *J. Phys.: Condens. Matter* **7**, 307 (1995).
- [12] P. S. Riseborough, *Phys. Rev. B* **68**, 235213 (2003).
- [13] J. C. Cooley, M. C. Aronson, Z. Fisk, and P. C. Canfield, *Phys. Rev. Lett.* **74**, 1629 (1995).
- [14] V. N. Antonov, B. N. Harmon, and A. N. Yaresko, *Phys. Rev. B* **66**, 165209 (2002).
- [15] P. Thunström, I. Di Marco, A. Grechnev, S. Lebègue, M. I. Katsnelson, A. Svane, and O. Eriksson, *Phys. Rev. B* **79**, 165104 (2009).
- [16] J. Yamaguchi, A. Sekiyama, M. Y. Kimura, H. Sugiyama, Y. Tomida, G. Funabashi, S. Komori, T. Balashov, W. Wulfhchel, T. Ito, S. Kimura, A. Higashiya, K. Tamasaku, M. Yabashi, T. Ishikawa, S. Yeo, S.-I. Lee, F. Iga, T. Takabatake, and S. Suga, *New J. Phys.* **15**, 043042 (2013).
- [17] A. Akabari and P. Thalmeier, *J. Korean Phys. Soc.* **62**, 1418 (2012).
- [18] K. S. Nemkovski, J. -M. Mignot, P. A. Ivanov, E. V. Nefedova, A. V. Rybina, L. -P. Regnault, F. Iga, and T. Takabatake, *Phys. Rev. Lett.* **99**, 137204 (2007).
- [19] T. Willers, B. Fåk, N. Hollmann, P. O. Körner, Z. Hu, A. Tanaka, D. Schmitz, M. Enderle, G. Lapertot, L. H. Tjeng, and A. Severing, *Phys. Rev. B* **80**, 115106 (2009).
- [20] P. Hansmann, A. Severing, Z. Hu, M. W. Haverkort, C. F. Chang, S. Klein, A. Tanaka, H. H. Hsieh, H.-J. Lin, C. T. Chen, B. Fåk, P. Lejay, and L. H. Tjeng, *Phys. Rev. Lett.* **100**, 066405 (2008).
- [21] T. Willers, Z. Hu, N. Hollmann, P. O. Körner, J. Gergner, T. Burnus, H. Fujiwara, A. Tanaka, D. Schmitz, H. H. Hieh, H.-J. Lin, C. T. Chen, E. D. Bauer, J. L. Sarro, E. Goremychkin, M. Koza, L. H. Tjeng, and A. Severing, *Phys. Rev. B* **81**, 195114 (2010).
- [22] T. Willers, D. T. Adroja, B. D. Rainford, Z. Hu, N. Hollmann, P. O. Körner, Y.-Y. Chin, D. Schmitz, H. H. Hieh, H.-J. Lin, C. T. Chen, E. D. Bauer, J. L. Sarro, K. J. McClellan, D. Byler, C. Geibel, F. Steglich, H. Aoki, P. Lejay, A. Tanaka, L. H. Tjeng, and A. Severing, *Phys. Rev. B* **85**, 035117 (2012).
- [23] T. Mori, S. Kitayama, Y. Kanai, S. Naimen, H. Fujiwara, A. Higashiya, K. Tamasaku, A. Tanaka, K. Terashima, S. Imada, A. Yasui, Y. Saitoh, K. Yamagami, K. Yano, T. Matsumoto, T. Kiss, M. Yabashi, T. Ishikawa, S. Suga, Y. Ōnuki, T. Ebihara, and A. Sekiyama, *J. Phys. Soc. Jpn.* **83**, 123702 (2014).
- [24] K. W. H. Stevens, *Proc. Phys. Soc. London Sect. A* **65**, 209 (1952).
- [25] B. T. Thole, G. van der Laan, J. C. Fuggle, G. A. Sawatzky, R. C. Karnatak, and J.-M. Esteve, *Phys. Rev. B* **32**, 5107 (1985).
- [26] A. Tanaka and T. Jo, *J. Phys. Soc. Jpn.* **63**, 2788 (1994).
- [27] R. D. Cowan, *The Theory of Atomic Structure and Spectra* (University of California Press, Berkeley, 1981).
- [28] A. Sekiyama, J. Yamaguchi, A. Higashiya, M. Obara, H. Sugiyama, M. Y. Kimura, S. Suga, S. Imada, I. A. Nekrasov, M. Yabashi, K. Tamasaku, and T. Ishikawa, *New J. Phys.* **12**, 043045 (2010).
- [29] A. Sekiyama, A. Higashiya, and S. Imada, *J. Electron Spectrosc. Relat. Phenom.* **190**, 201 (2013).
- [30] M. Yabashi, K. Tamasaku, and T. Ishikawa, *Phys. Rev. Lett.* **87**, 140801 (2001).
- [31] H. Fujiwara, S. Naimen, A. Higashiya, Y. Kanai, H. Yomosa, K. Yamagami, T. Kiss, T. Kadono, S. Imada, A. Yamasaki, K. Takase, S. Otsuka, T. Shimizu, S. Shinbara, S. Suga, M. Yabashi, K. Tamasaku, T. Ishikawa, and A. Sekiyama, arXiv:1505.04591.
- [32] A. Czopnik, N. Shitsevalova, A. Krivchikov, Y. Paderno, and Y. Onuki, *J. Phys.: Condens. Matter* **17**, 5971 (2005).